Electronic Supplementary Material (ESI) for Journal of Materials Chemistry C.

Electronic Supplementary Information for

Purely organic Vis-to-UV upconversion with an excited annihilator singlet beyond 4 eV

Till J. B. Zähringer[a], Maria-Sophie Bertrams[a] and Christoph Kerzig[a]

[a] Department of Chemistry, Johannes Gutenberg University Mainz, Duesbergweg 10—14, 55128 Mainz, Germany.

Correspondence: ckerzig@uni-mainz.de

Contents

1 General experimental details and methods

Materials

Unless otherwise noted, all chemicals used for optical spectroscopy, preparative and irradiation experiments were obtained commercially in high purity and used as received (4-bromobiphenyl, 98%, Alfa Aesar; 3-bromobiphenyl, 99%, Alfa Aesar; 2-bromobiphenyl, 98%, Alfa Aesar; (triisopropylsilyl)acetylene, 97%, Alfa Aesar; bis(triphenylphosphine)palladium(II) dichloride, 98%, Acros Organics; copper(I) iodide, 99.9%, Alfa Aesar; triphenylphosphine, 99%, Sigma-Aldrich; diisopropylamine, 99.9%, VWR Chemicals; *fac*-Ir(4′,6′-dFppy)$_3$ (**IrdF**), 98%, Sigma-Aldrich; 2,4,5,6-tetrafluoro-1,3-benzenedicarbonitrile, 97%, Alfa Aesar; carbazole, 95%, Alfa Aesar; sodium-bis(trimethylsilyl)amide 2 M in THF, 99.7%, Alfa Aesar; *p*-terphenyl, 98%, Alfa Aesar; biphenyl, 99.5%, Sigma-Aldrich; perylene, 98%, Alfa Aesar; ethanol, 99.8%, VWR Chemicals; cyclohexane, 99.7%, VWR Chemicals; acetonitrile, 99.7%, Sigma-Aldrich; sodium sulfate, 99%, Acros Organics; diethyl ether, 99.5%, Fisher Scientific; heptane, 99%, Sigma-Aldrich; chloroform, 99%, Carl Roth). Argon from Nippon Gases (5.0) was used for removing dissolved oxygen prior to all experiments related to optical spectroscopy.

Steady-state measurements

Absorption spectra were recorded using a LAMBDA 365 instrument from Perkin Elmer. Emission measurements were carried out with a Perkin Elmer FL-6500 spectrometer. All steady-state absorption and emission measurements were performed at room temperature (295 ± 2 K) and the emission spectra were corrected for the wavelength-dependent sensitivity of the instrument. Very low concentrations of the emissive compounds were employed to avoid filter effects. The singlet-excited state energies were determined by the intersection points of the respective normalized fluorescence and the absorption spectra. The triplet energy of **IrdF** was estimated from the short-wavelength edge of its room-temperature emission spectrum, where the emission intensity drops to 10 % compared to the global maximum.

Determination of fluorescence quantum yields

The fluorescence quantum yields of the annihilators were determined by comparing their fluorescence spectra with those of a reference system ref (*p*-terphenyl in cyclohexane, Φ_{FL} = 0.93).[1] The quantum yield was then calculated using equation (1.1), where Φ_{FL} represents the quantum yield, *I* the integrated fluorescence intensity, *A* the absorption at the incident wavelength and the refractive index of the solvent *n* taken from ref.[1]. All solutions were adjusted to an optical density below 0.1 at the irradiation wavelengths to avoid filter effects. The fluorescence quantum yield of **4CzIPN** in cyclohexane/toluene (9:1) was determined by comparing the fluorescence to a reference quantum yield of **4CzIPN** in toluene, averaged from literature values (see Table S2).[2,3] The emission quantum yield of **IrdF** was determined using perylene in ethanol (Φ_{FL} = 0.92)[1] as reference system. Three independent quantum yield determinations were carried out and averaged for each annihilator or sensitizer.

$$\Phi_{\mathrm{Fl}} = \Phi_{\mathrm{Fl,ref}} \cdot \frac{I}{I_{\mathrm{ref}}} \cdot \frac{A_{\mathrm{ref}}}{A} \cdot \frac{n^2}{n_{\mathrm{ref}}^2} \tag{1.1}$$

Upconversion efficiency measurements

The power dependent upconversion measurements were conducted with a 447 nm cw laser (Roithner Lasertechnik, optical output: up to 1.1 W, see Figure S2 for the data sheet) with adjustable power output and a beam size of ~0.10 cm^2 or a 440 nm LED (Kessil Science, PR160L) with four power settings (25, 50, 75, and 100%). The average intensity of the LED (at 100% output power) is reported as 352 mW·cm^{-2} (measured from 1 cm distance).[4] The emission spectra were measured by irradiating a water-containing cuvette in the FL-6500 instrument and they are displayed in Figure S1. The light source was installed in a 90° angle with respect to the detector. The LED intensity and laser output was further attenuated with neutral density filters obtained from Newport (ND2.0, ND1.0, ND0.5, ND0.3, ND0.1).

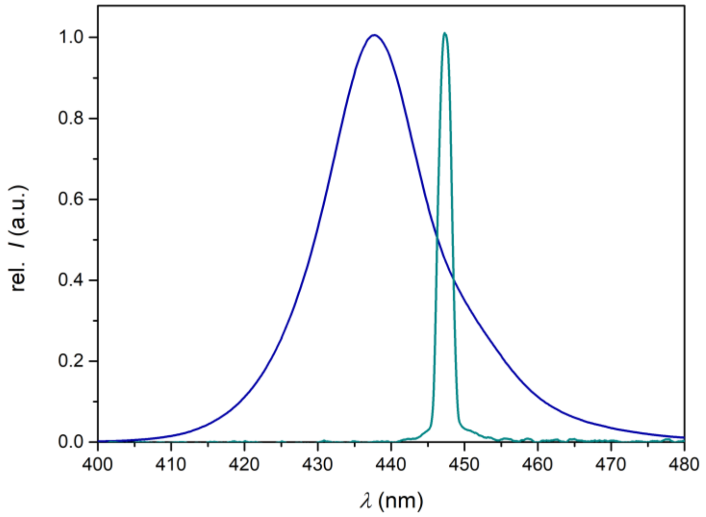

Figure S1: Emission spectrum of the PR160L 440 nm LED from Kessil Science (blue) and the 447 nm cw laser from Roithner Lasertechnik (green). The emission spectrum was measured by irradiating a water-containing cuvette in the emission spectrometer.

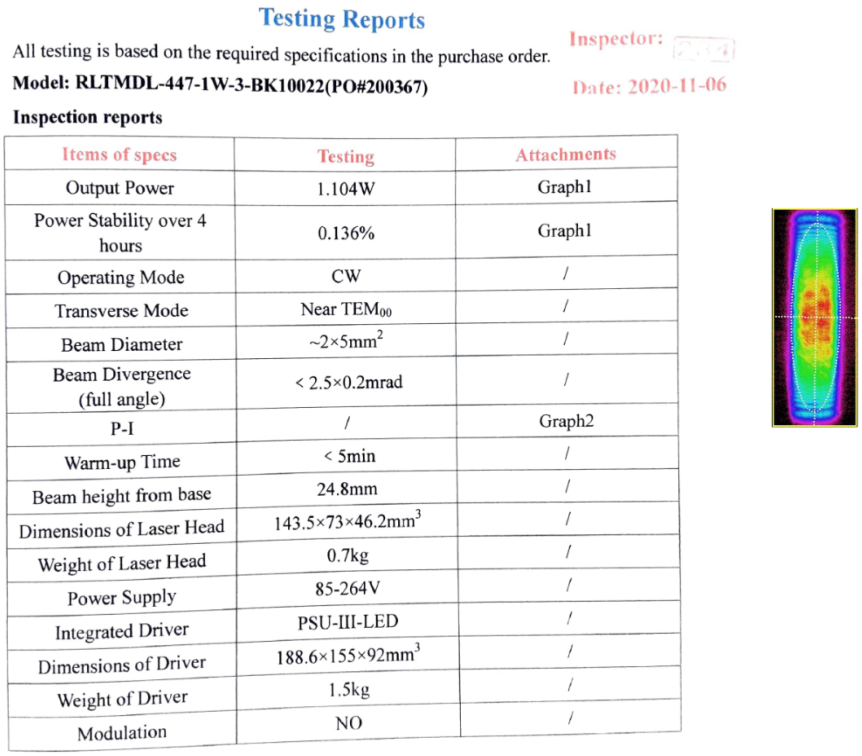

Testing Reports

All testing is based on the required specifications in the purchase order.

Inspector:

Model: RLTMDL-447-1W-3-BK10022(PO#200367)

Date: 2020-11-06

Inspection reports

Items of specs	Testing	Attachments
Output Power	1.104W	Graph1
Power Stability over 4 hours	0.136%	Graph1
Operating Mode	CW	/
Transverse Mode	Near TEM_{00}	/
Beam Diameter	~2×5mm^2	/
Beam Divergence (full angle)	< 2.5×0.2mrad	/
P-I	/	Graph2
Warm-up Time	< 5min	/
Beam height from base	24.8mm	/
Dimensions of Laser Head	143.5×73×46.2mm^3	/
Weight of Laser Head	0.7kg	/
Power Supply	85-264V	/
Integrated Driver	PSU-III-LED	/
Dimensions of Driver	188.6×155×92mm^3	/
Weight of Driver	1.5kg	/
Modulation	NO	/

Figure S2: Data sheet of the 447 nm cw laser from Roithner Lasertechnik and a typical beam profile (right) for the RLTMDL-447-1W laser series provided by the manufacturer.

Upconversion quantum yields

The quantum yields of the UC systems were estimated by the ratios of (integrated) upconverted photons generated relative to the integrated emission of a reference system with a well-known quantum yield. For that, the photoluminescence intensity of a reference solution containing the very same sensitizer in the absence of the annihilator was measured under identical conditions as the complete upconversion system. In some measurements, a neutral density filter from Newport was used to attenuate the luminescence signal in order to avoid over-saturation of the detector. The following reference quantum yields were used: **IrdF** in Ar-saturated MeCN, $\Phi = 0.61 \pm 0.03$; **4CzIPN** in deoxygenated cyclohexane/toluene (9:1), $\Phi = 0.90 \pm 0.01$.

The upconversion quantum yields presented herein have not been multiplied by two (theoretical maximum of 50 %).

Triplet energy transfer rates (quenching rate constants)

The quenching constants were determined from Stern-Volmer experiments. The lifetime of the sensitizer was measured with different concentrations c_q of ***p*-TIPS-BP** and fitted in Stern-Volmer plots according to equation (1.2). With the unquenched lifetime the quenching rate constant was derived from the corresponding Stern-Volmer constant K_{SV}.

$$\frac{\tau_0}{\tau} = \frac{\Phi_0}{\Phi} = \frac{\mathrm{F}_0}{\mathrm{F}} = 1 + \tau_0 \cdot k_\mathrm{q} \cdot c_\mathrm{q} = 1 + K_\mathrm{SV} \cdot c_\mathrm{q} \tag{1.2}$$

Stokes shift determinations

The Stokes shifts were estimated from the absorption and emission spectra. The shift was obtained by the “distance” between the absorption peak with the lowest wavenumber and the emission peak with the highest wavenumber as displayed in Figure S8. The results are summarized in Table S3.

Laser flash photolysis

The LP980KS setup from Edinburgh Instruments equipped with an Nd:YAG laser from Litron (Nano LG 300-10) was employed for transient absorption spectroscopy. The frequency-tripled output with a wavelength of 355 nm served as excitation source. The laser pulse duration was ~5 ns and the pulse frequency was 10 Hz. The typical pulse energy used for transient absorption and emission studies was 15 mJ. Detection of transient absorption spectra occurred on an iCCD camera from Andor. Single-wavelength kinetics were recorded using a photomultiplier tube. The spectroscopic experiments were performed at 293 K using a cuvette holder that allows temperature control. If not stated otherwise the TA spectra were integrated over 100 ns.

Fluorescence lifetime measurements

Fluorescence lifetime measurements with ***p*-TIPS-BP** were performed on a Lifespec II spectrometer (time-correlated single photon counting (TCSPC) technique) from Edinburgh Instruments using a pulsed LED (ca. 900 ps pulse width) for excitation at 313 nm. The unquenched lifetime was recorded at 293 K with a highly diluted solution (containing less than 0.1 mM ***p*-TIPS-BP** in MeCN) to avoid self-quenching (Figure S15).

Chromatography

For standard liquid column chromatography separation silica gel 60 M (0.040-0.063 mm Macherey-Nagel GmbH & Co., Düren, Germany) was used.

Thin-layer-chromatography was performed using “DC Kieselgel 60 F254” (Merck KGaA, Darmstadt, Germany) on aluminum and a UV lamp (Benda, NU-4 KL, λ = 254 nm, and 365 nm, Wiesloch, Germany) was employed for detection. The resulting R_f values are given relative to the solvent.

NMR spectroscopy

For NMR spectroscopy a multi nuclear magnetic resonance spectrometer of the type AV II 400 (Bruker, analytic measuring technique, Karlsruhe, Germany) was employed. The chemical shifts are given as δ-values in ppm and they were referenced relative to the residue signal of the non-deuterated solvent.[5] The following abbreviations were used: singlet (s), doublet (d), multiplet (m), and the coupling constant (J).

Mass spectrometry

Accurate mass spectrometry was carried out with a G6545A Q-ToF (Agilent GmbH, Waldbronn, Germany) instrument using the photoionization at atmospheric pressure (APPI) technique. The sample was injected *via* a 1260 Infinity II HPLC system (Agilent GmbH, Waldbronn, Germany) with a G7111B 1260 quaternary pump, a G7129A 1260 vial sampler, and a G7116A 1260 multicolumn thermostat. Mass calibration was performed on the same day of the actual measurement using an external standard. The mass accuracy of the measurements is expected to be better than 5 ppm.

Preparation of deoxygenated solutions for photon upconversion studies

Unless noted otherwise, the solutions for photon upconversion experiments were deoxygenated in custom-made Schlenk-cuvettes (Figure S3) by five freeze-pump-thaw cycles using Argon as an inert gas, liquid N_2 for cooling, and Schlenk line vacuum (down to 0.5 mbar). The control experiments and the findings presented in Chapter 8 show that this method was sufficient to remove practically all oxygen from the solutions, given that remaining oxygen traces (probably below or on the order of ~0.02 mM, which is two orders of magnitude lower than in air-saturated solutions) will be removed by our annihilator (see Chapter 8 for details).

Figure S3: Photograph of a Schlenk-cuvette used for the preparation of deoxygenated solutions for photon upconversion studies.

2 Synthetic procedures

2.1 Synthesis of TIPS-ethynylated biphenyls

The synthesis proceeds *via* the Sonogashira coupling reaction analogous to the preparation of other TIPS-functionalized aromatic compounds.[6] The exact quantities are listed for each TIPS-biphenyl derivative below. Bromo-biphenyl, $Pd(PPh_3)_2Cl_2$, CuI, PPh_3, and dry THF were added to a round-bottom flask under argon flow. The flask was equipped with a condenser column and diisopropylamine was added to the solution under constant stirring. The flask was heated to 70˚C and (triisopropylsilyl)acetylene was added dropwise to the mixture. The mixture was held at 70˚C over night under argon atmosphere. The completion of the reaction was tested with thin layer chromatography (TLC). After cooling the mixture was filtered and the solvent was then removed under reduced pressure. The residue was redissolved in chloroform. The product was washed twice with deionized water and twice with brine. The organic layer was dried with Na_2SO_4 and the solvent was removed under reduced pressure. The product was purified via column chromatography (cyclohexane). The three TIPS-biphenyl isomers have already been prepared previously.[7] However, we stress that these studies focused on novel coupling reactions and the photophysical properties of the three compounds were completely unexplored prior to our work. NMR data (see below) of all biphenyl derivatives are in agreement with those reported in the literature.[7]

***p*-TIPS-BP**: 5 g 4-Bromobiphenyl (21.5 mmol), 182 mg $Pd(PPh_3)_2Cl_2$ (0.26 mmol), 131 mg CuI (0.69 mmol), 181 mg PPh_3 (0.69 mmol) and 170 mL dry THF, 72 mL diisopropylamine, 10 mL (triisopropylsilyl)acetylene (44.5 mmol); yield = 2.38 g, 7.1 mmol (33%).

R_f(cyclohexane) = 0.5

APPI-HRMS (m/z): calculated for $[M + H]^+$: 335.2190, found 335.2185.

^{1}H NMR (400 MHz, $CDCl_3$): δ [ppm] = 7.60-7.57 (m, 2H), 7.56-7.52 (m, 4H), 7.47-7.43 (m, 2H), 7.38-7.34 (m, 1H), 1.15 (pseudo-s, 21H).

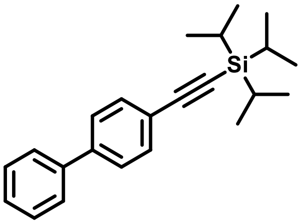

***m*-TIPS-BP**: 1 g 3-Bromobiphenyl (4.3 mmol), 36.5 mg $Pd(PPh_3)_2Cl_2$ (0.052 mmol), 26.2 mg CuI (0.14 mmol), 36.1 mg PPh_3 (0.14 mmol), 28 mL dry THF, 13.5 mL diisopropylamine, 1.85 mL (triisopropylsilyl)acetylene (8.2 mmol); yield = 0.79 g, 2.3 mmol (55%).

R_f(cyclohexane) = 0.5

APPI-HRMS: Unfortunately, no signal directly related to the complete molecule could be detected with this method. However, the mass spectrum of the compound shows two characteristic fragments that give the complete molecule signal (and both fragments are also detectable for ***p*-TIPS-BP**).

m/z: $[C_{14}H_{11}]^+$, calculated 179.0856, found 179.0855; $[SiC_9H_{21}]^+$, calculated 157.1407, found 157.1408; sum of both fragments with adducts removed $[C_{23}H_{30}Si]^+$, calculated 334.2117, found 334.2117.

^{1}H NMR (400 MHz, $CDCl_3$): δ [ppm] = 7.70-7.69 (m, 1H), 7.60-7.51 (m, 3H), 7.48-7.33 (m, 5H), 1.15 (pseudo-s, 21H).

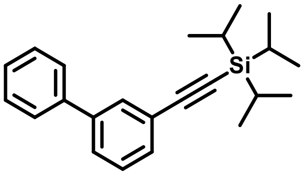

***o*-TIPS-BP**: 1 g 2-Bromobiphenyl (4.3 mmol), 36.5 mg $Pd(PPh_3)_2Cl_2$ (0.052 mmol), 26.2 mg CuI (0.14 mmol), 36.1 mg PPh_3 (0.14 mmol), 28 mL dry THF, 12.5 mL diisopropylamine, 1.85 mL (triisopropylsilyl)acetylene (8.2 mmol); yield = 0.88 g, 2.6 mmol (61%).

R_f(cyclohexane) = 0.5

APPI-HRMS: Unfortunately, no signal directly related to the complete molecule could be detected with this method. However, the mass spectrum of the compound shows two characteristic fragments that give the complete molecule signal (and both fragments are also detectable for ***p*-TIPS-BP**).

m/z: $[C_{14}H_{11}]^+$, calculated 179.0856, found 179.0854; $[SiC_9H_{21}]^+$, calculated 157.1407, found 157.1406; sum of both fragments with adducts removed $[C_{23}H_{30}Si]^+$, calculated 334.2117, found 334.2119.

^{1}H NMR (400 MHz, $CDCl_3$): δ [ppm] = 7.62-7.57 (m, 3H), 7.40-7.27 (m, 6H), 1.01 (pseudo-s, 21H).

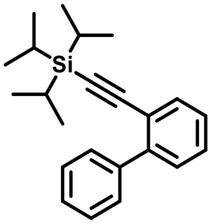

2.2 Synthesis of 4CzIPN

The compound **4CzIPN** was synthesized according to a literature report.[8] A flame-dried 100 mL three neck round flask was charged with 3.68 g (22 mmol) carbazole under argon flow. The flask was evacuated for 5 min and then filled with argon three times. 50 mL THF were added to the flask, which was then cooled to 0˚C in an ice-water bath for 10 min. 10.5 mL (21 mmol) 2 M sodium-bis(trimethylsilyl)amide in THF was added dropwise over 5 min. The ice bath was removed after 5 min, and the solution was stirred at room temperature for 30 min. 1 g (5 mmol) 2,4,5,6-tetrafluoro-1,3-benzenedicarbonitrile was solved in 4 mL dry THF and added dropwise under argon flow to the solution. The solution was heated to 70°C for 24 h. The solvent was then removed under reduced pressure. The residue was washed with 100 mL diethyl ether. The product was extracted with 100 mL chloroform from the filter cake. The solvent was removed under reduced pressure and the residue was washed with *n*-heptane. Yield: 3.54 g, 4.5 mmol (90%). The compound was then further purified by sublimation prior to its use as sensitizer. The NMR spectrum is in agreement with that reported in the literature.[3]

^{1}H NMR (400 MHz, $CDCl_3$): δ [ppm] = 8.22(d, J_{HH} = 8 Hz, 2H), 7.74-7.67 (m, 8H), 7.51-7.47 (m, 2H), 7.33 (d, J_{HH} 8 Hz, 2H), 7.23-7.21 (m, 4H), 7.12-7.05 (m, 8H) 6.84-6.80 (m, 4H), 6.65-6.61 (m, 2H).

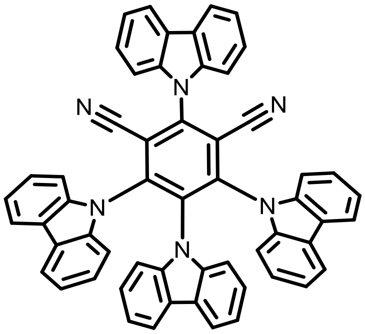

3 DFT calculations

Table S1: Computed triplet energies (in eV or kJ/mol) for biphenyl and corresponding TIPS-derivatives. Details are given in the text below.

Derivative	E_T (calc.) [a] [eV]	E_T (lit.) [b] [eV]	E_T (cor.) [c] [eV]	E_T (cor.) [d] [kJ mol^{-1}]
biphenyl (**BP**)	2.99	2.84	–	274
***p*-TIPS-BP**	2.61	–	2.48	239
***m*-TIPS-BP**	2.97	–	2.83	273
***o*-TIPS-BP**	2.82	–	2.68	259

[a] DFT-calculated triplet energy at the B3LYP/6-311+G(d,p) level of theory. [b] Experimental triplet energy taken from ref.[1]. [c] Calculated triplet energy corrected for overestimation (value from [a] multiplied by 0.95). [d] Value from [b] or [c] converted in kJ mol^{-1}.

All DFT calculations were carried out with the Gaussian 09 software package[9] using the B3LYP functional in combination with the 6-311+G(d,p) basis set. The geometry optimizations of biphenyl and their TIPS derivatives under study were accompanied by frequency analyses. The optimized structures used for further computations did not show negative vibrational frequencies, indicating convergence on minimum structures. Starting from the energy-minimized singlet ground state geometries, the corresponding lowest triplet states were calculated. The triplet state energies were determined simply by comparing the energies of both optimized structures (i.e., singlet ground state and triplet state) for a given compound since this straightforward approach has proven very successful for predicting the triplet energies for several organic chromophores.[6,10,11] A spin density map was obtained by an additional single-point calculation with population analysis and time-dependent DFT computations with identical functional and basis were used to calculate the vertical excitation energies for simulating the triplet-triplet absorption spectrum of ***p*-TIPS-BP**. The calculated triplet absorption spectrum shows a maximum at 420 nm, which is in good agreement with the experimental triplet absorption spectrum peaking at 408 nm. The representative optimized structure and the spin density distribution of the triplet are displayed in Figure S4.

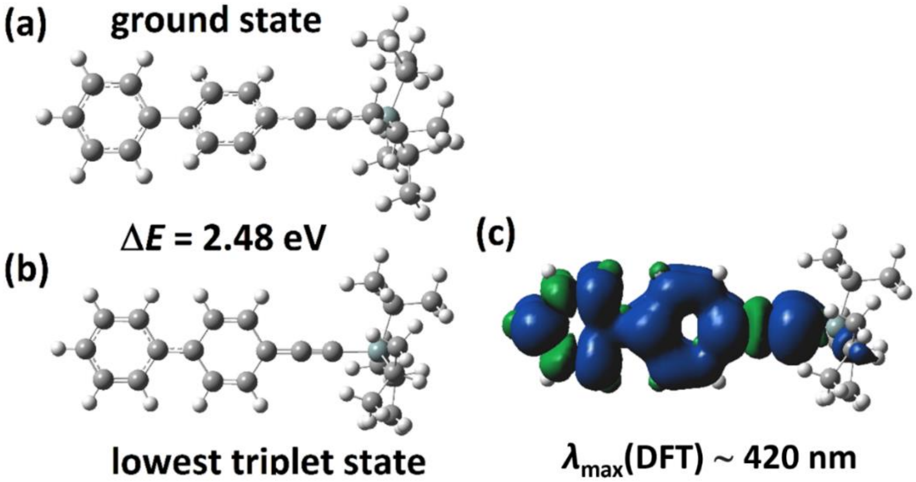

Figure S4: Optimized structures of the singlet ground state (a) as well as the lowest triplet state (b) of *p*-TIPS-BP at the B3LYP/6-311+G(d,p) level of theory, together with the corresponding energy difference (i.e., the estimated triplet energy of p-TIPS-BP). (c) Computed spin densities of the triplet state using the same computational method. Its absorption maximum estimated by TD-DFT is also displayed in subfigure (c). Blue colour represents positive spin densities, whereas green represents negative spin densities.

The computed triplet energies E_T are summarized in Table S1. The calculated triplet energy for the reference compound biphenyl is higher than its literature-known experimental triplet energy by ~5 %. Therefore, we adjusted the computed energies of all compounds with unknown triplet states by a correction factor of 0.95.

4 *Solvent dependence of 4CzIPN's photochemical properties*

The singlet- and triplet-excited state energies as well as the intersystem crossing quantum yield, Φ_{ISC}, and prompt/delayed fluorescence properties of **4CzIPN** show a pronounced solvent dependence. The singlet-excited state energy and Φ_{ISC} decrease as the polarity of the solvent increases.[12] We speculated that a highly nonpolar solvent like cyclohexane would yield the highest singlet and triplet energies. However, **4CzIPN** dissolves very poorly in neat cyclohexane. We, therefore, added 10vol% of toluene as co-solvent (when higher **4CzIPN** concentrations are required) giving us the best compromise between solubility and excited-state energies (Figure S5). The overall fluorescence quantum yield Φ_{Fl} was practically identical in our solvent mixture compared to neat toluene (compare, Table S2). Moreover, time-gated emission spectra recorded with our LFP setup revealed that the ratio of prompt and delayed fluorescence is almost completely unaffected. Hence, we concluded that the reported ISC quantum yield (Φ_{ISC} = 0.73 in toluene[12]) must be very similar in our system. Further, the triplet-excited state energy of **4CzIPN** in cyclohexane was estimated by subtracting the singlet-triplet energy gap in toluene (0.04 eV)[2] from the experimental singlet-excited state energy in cyclohexane (2.76 eV, see Table S2).

Table S2: Photophysical properties of **4CzIPN** in toluene and cyclohexane.

Compound	S_1 [eV]	T_1 [eV]	Φ_{Fl}	Φ_{ISC}	τ_T[f] [µs]
4CzIPN	2.71[a] 2.76[b]	2.67[a] 2.72[c]	0.90[a] 0.90±0.01[d]	0.73[e]	4.6[a] 7.9[d]

[a] Measured in toluene from ref.[2,3]. [b] Measured in cyclohexane [c] Estimated for cyclohexane from the singlet-triplet energy gap in toluene. [d] Measured in cyclohexane/toluene (9:1). [e] Measured in toluene from ref.[12]. [f] Triplet lifetime.

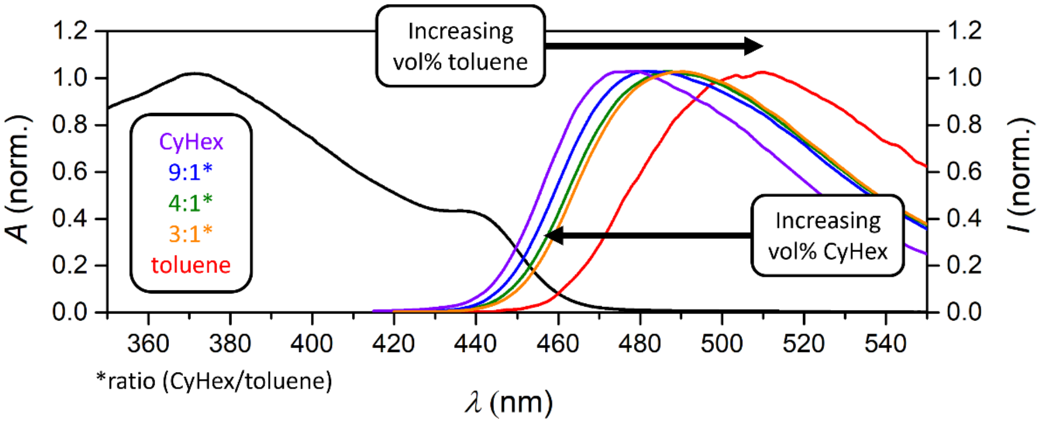

Figure S5: Absorption and photoluminescence spectrum of 4CzIPN dissolved in different ratios of cyclohexane and toluene. Absorption (norm.): cyclohexane (black). Photoluminescence (cyclohexane:toluene ratio): neat cyclohexane (purple); 9:1 (blue); 4:1 (green); 3:1 (orange); neat toluene (red). The position of the absorption peak is not affected by the addition of toluene.

5 *Photostability of the upconversion system*

In order to provide evidence for the applicability of this novel annihilator and the resulting UC system, we irradiated a solution containing 44 µM **4CzIPN** and 10 mM ***p*-TIPS-BP** with a cw laser at 447 nm employing a power density of 1.5 W·cm^{-2}, corresponding to the threshold intensity I_{th} (see Figure 5 of the main paper). The UC system shows decent photostability (Figure S6), taking the rather high laser power into account. Consequently, the UC signal is expected to decrease more quickly than observed for similar systems with less highly energetic excited annihilators.[13,14]

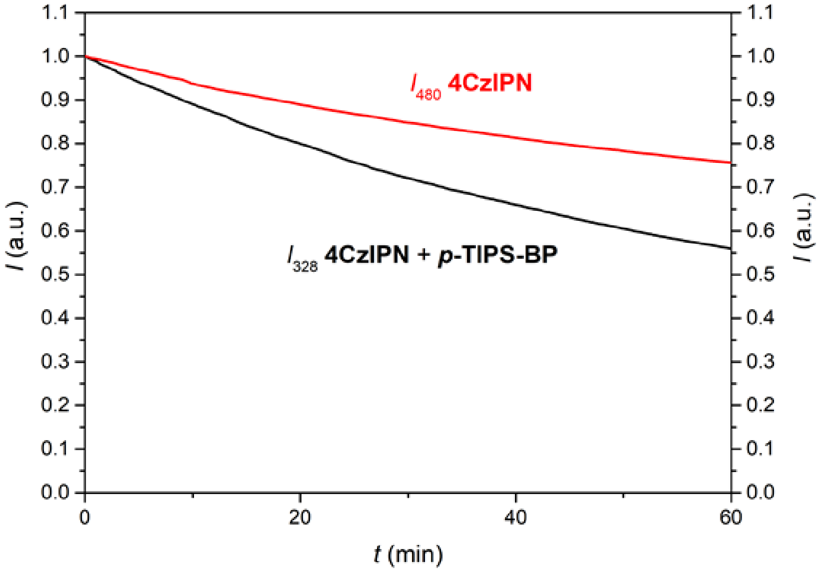

Figure S6: Upconversion/sensitizer emission stability measurements over one hour in cyclohexane/toluene (9:1) using a cw laser for excitation at 447 nm and a constant laser power of 1.5 W·cm^{-2}. Black curve: Emission intensity of a deoxygenated solution containing 44 µM **4CzIPN** *and* 10 mM ***p*-TIPS-BP** with detection at 328 nm. Red curve: Emission intensity of a deoxygenated solution containing 44 µM **4CzIPN** monitored at 480 nm.

6 UV filter effects caused by the sensitizer

Despite the slightly higher triplet quenching efficiency of ***p*-TIPS-BP** with **IrdF** compared to **4CzIPN** (96% vs. 92% with 10 mM of the annihilator) as well as its higher ISC quantum yield and the higher fluorescence quantum yield of the annihilator in MeCN than in cyclohexane (83 ± 2% vs. 48 ± 2%), the UC system **4CzIPN**/***p*-TIPS-BP** (in cyclohexane) has a much higher overall quantum yield (compare, Figure 5 and Figure S13). This probably originates from the very different (relative) absorption properties of both sensitizers at the excitation wavelength and in the UV region, where the annihilator emits. The absorption of **4CzIPN** in the wavelength range of the upconverted emissions (300-380 nm) is about twice as large as at the incident wavelength (λ_{ex} = 447 nm). In contrast, the molar absorptivity ε of **IrdF** increases by more than one order of magnitude (Figure S7) with λ_{ex} as reference point. The strong reabsorptivity of upconverted photons by the sensitizer[15] ("optical loss") is expected to decrease the external quantum yield Φ_{UC} significantly in this case.

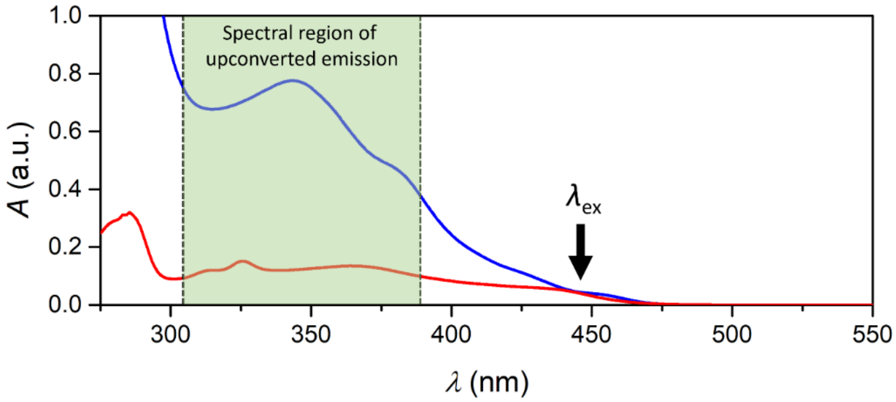

Figure S7: Normalized (at 447 nm) absorption spectra of **4CzIPN** (red) and **IrdF** (blue). The spectra were adjusted to visualize the high reabsorption of **IrdF**. The molar absorptivity of **4CzIPN** rises only slightly from the incident wavelength (λ = 447 nm) to the UV region (300-380 nm). Compared to that, the molar absorptivity of **IrdF** increases more than one order of magnitude resulting in strong reabsorption of the upconverted light.

7 Photophysical properties of biphenyl (BP), p-TIPS-BP, o-TIPS-BP, and m-TIPS-BP

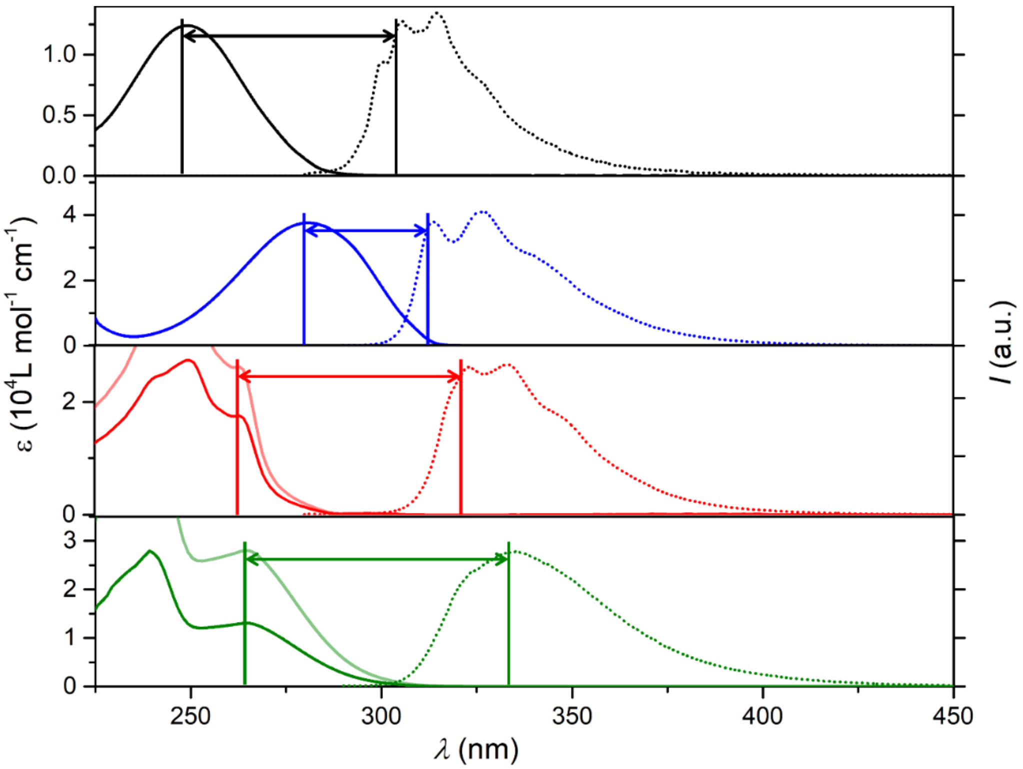

Figure S8: Absorption (solid lines) and normalized photoluminescence (dotted lines) spectra of biphenyl[a] (black), ***p*-TIPS-BP**[a] (blue), ***m*-TIPS-BP**[b] (red), ***o*-TIPS-BP**[b] (green). For clarity, the absorption spectra of ***o*-TIPS-BP** and ***m*-TIPS-BP** are displayed with and without a scaling factor. Vertical lines indicate the wavelengths used for Stokes shift determinations. [a] Measured in MeCN. [b] Measured in THF.

Substituting biphenyl in the *ortho* and *meta* position (***m*-TIPS-BP** and ***o*-TIPS-BP**) did not show the same beneficial influence of the TIPS group as for ***p*-TIPS-BP**. The triplet-excited states of both lie too high (Table S1) for efficient sensitization by a blue-light absorbing sensitizer such as **4CzIPN** and **IrdF**. Further, the Stokes shift of ***m*-TIPS-BP** and ***o*-TIPS-BP** is not reduced, which would lead to a lower anti-Stokes shift in the resulting upconversion system (Figure S8). Table S3 compares pertinent photophysical properties of biphenyl and its TIPS derivatives under study.

Table S3: Measured S_1 energies, computed T_1 energies, fluorescence quantum yields Φ_{Fl} and Stokes shifts, $\Delta\tilde{\nu}$, of biphenyl and TIPS-biphenyls. The solvent choice had no major influence on the S_1 energy (see Figure S10 for an example).

Compound	S_1 [eV]	T_1 [eV]	Φ_{Fl}	$\Delta\tilde{\nu}$ [cm^{-1}]
Biphenyl (**BP**)	4.34[a] 4.34[b]	2.84[d]	0.18[f]	7480[a] 7860[b]
***p*-TIPS-BP**	4.04[a] 4.05[b] 4.03[c]	2.48[e]	0.83±0.02[a] 0.48±0.02[b]	3870[a] 3970[b]
***m*-TIPS-BP**	4.14[c]	2.83[e]	–	7060[c]
***o*-TIPS-BP**	4.09[c]	2.68[e]	–	8030[c]

[a] Measured in MeCN. [b] Measured in cyclohexane. [c] Measured in THF. [d] Experimental triplet energy taken from ref.[1]. [e] DFT-calculated triplet energy at the B3LYP/6-311+G(d,p) level of theory and corrected for overestimation. [f] Experimental fluorescence quantum yield in cyclohexane taken from ref.[16].

8 Control experiments related to residual oxygen during photon upconversion studies

Residual oxygen in solution can be regarded as a substantial problem for the performance of photon upconversion systems. Oxygen-scavenging additives have proven successful for complementing inert gas purging or freeze-pump-thaw cycles,[17] and specific solvents that permit air-stable photon upconversion have been identified.[18] However, some annihilators such as anthracene derivatives can efficiently remove dissolved oxygen through a sensitization-photoaddition sequence, in particular, if the annihilator concentration is much higher than that of oxygen.[19] We presume that traces of residual oxygen are depleted by our annihilator compound, which is typically used at a concentration of 10 mM, during the irradiation of our samples. To prove this comparative photon upconversion studies were performed with poorly deoxygenated solutions containing 44 µM **4CzIPN** and 10 mM ***p*-TIPS-BP** in cyclohexane:toluene (9:1) using a cw laser for excitation at 447 nm (OD_{447} = 0.2). The first solution was purged with argon via a needle for 60 s (blue curve, Figure S9). The upconverted emission signal at 328 nm increases slowly over 5 minutes before reaching its maximum, after turning on the cw laser. The second solution was only purged for 40 s with argon (green curve), corresponding to a higher concentration of dissolved oxygen in our solvent mixture. The UC signal resides at a very low intensity for 5 minutes before it slowly rises as well. However, neither a lag time nor an intensity increase is observed when proper Schlenk-techniques are used as described in Chapter 1 (e.g. for the measurements in Figure S6) implying that oxygen was removed very efficiently by our experimental procedure for sample preparation. We believe that the rising upconversion signal from the poorly deoxygenated solution stems from remaining concentrations of dissolved oxygen in solution quenching the triplet-excited states, thereby generating singlet oxygen. The latter in turn is slowly removed from the system by reacting with excess annihilator molecules in their ground states. In other words, after a short irradiation time, oxygen traces will be removed completely.

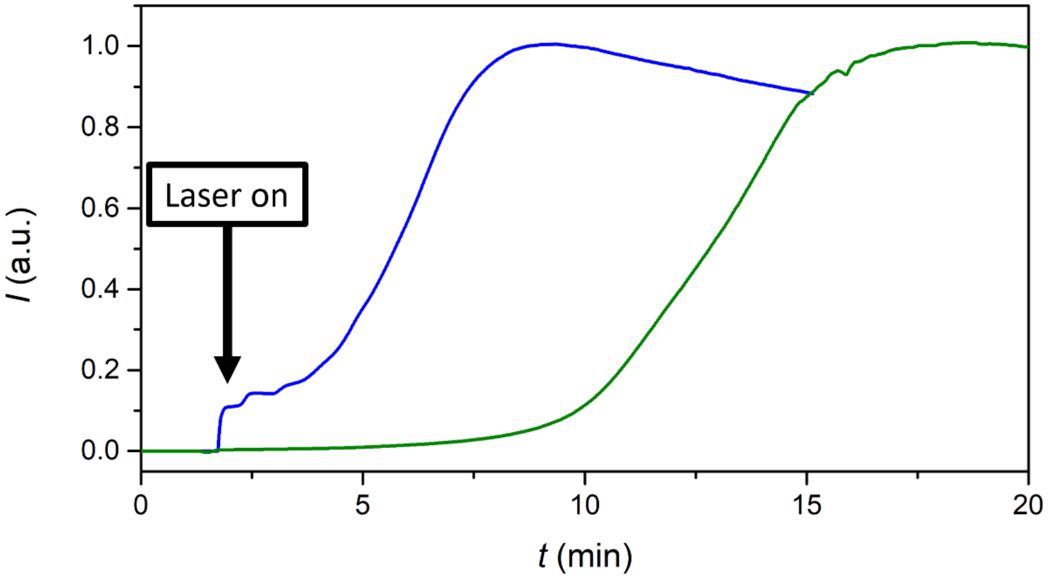

Figure S9: Photon upconversion studies with poorly deoxygenated solutions containing 44 µM **4CzIPN** and 10 mM ***p*-TIPS-BP** in cyclohexane:toluene (9:1) using a cw laser for excitation at 447 nm (OD_{447} = 0.2) with a laser power of 100 mW. The intensity of the upconversion signal was measured at 328 nm and recorded for several minutes. Blue curve: Flushed with argon for 60 s; green curve: Flushed with argon for 40 s. See text for further explanations.

9 *Additional spectroscopic data*

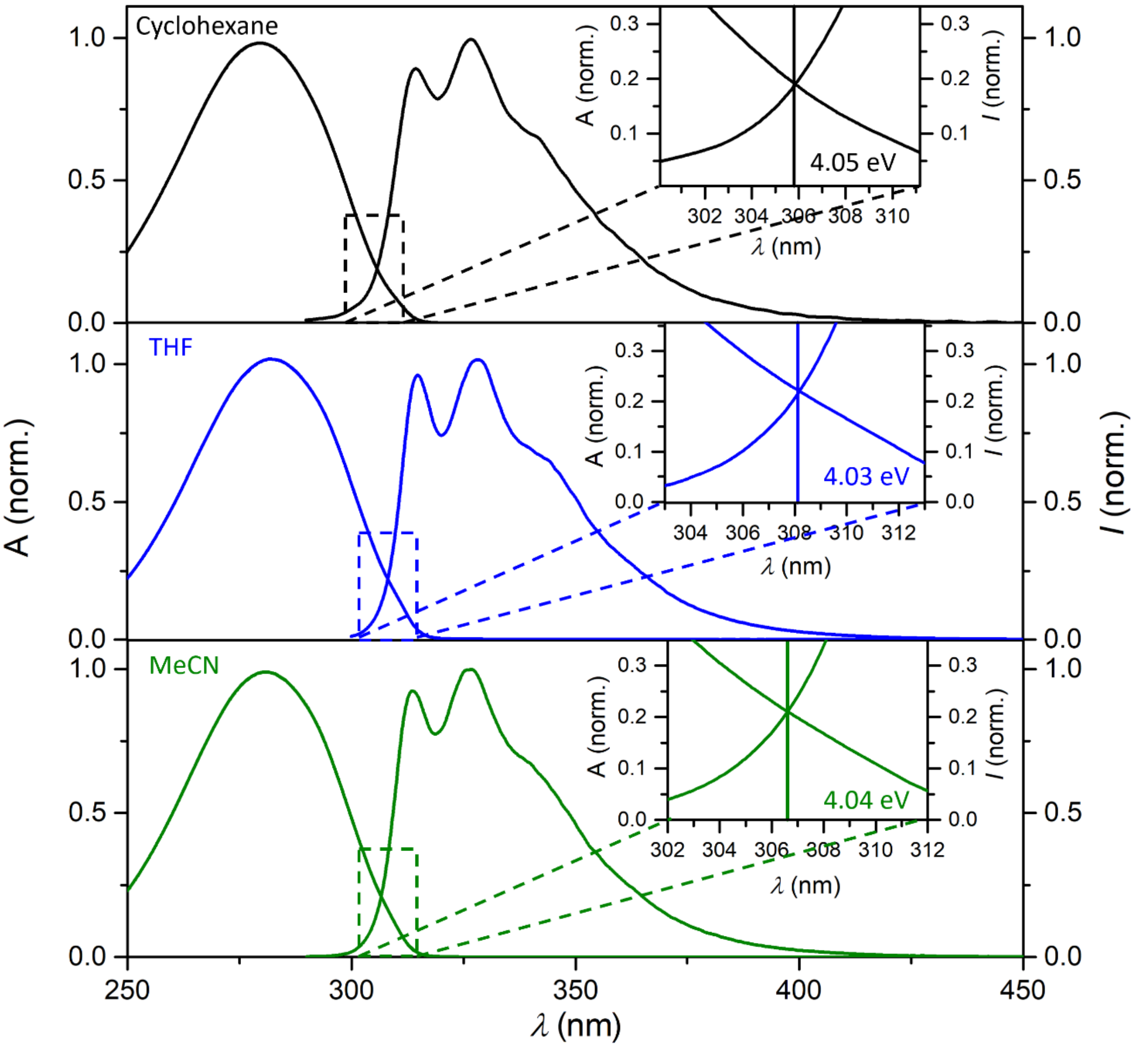

Figure S10: Normalized absorption and normalized emission spectra of ***p*-TIPS-BP** in different solvents: cyclohexane (black), THF (blue) and MeCN (green). Each inset shows the crossing point of normalized absorption and emission spectra on enlarged scale and the corresponding S_1 energy in eV.

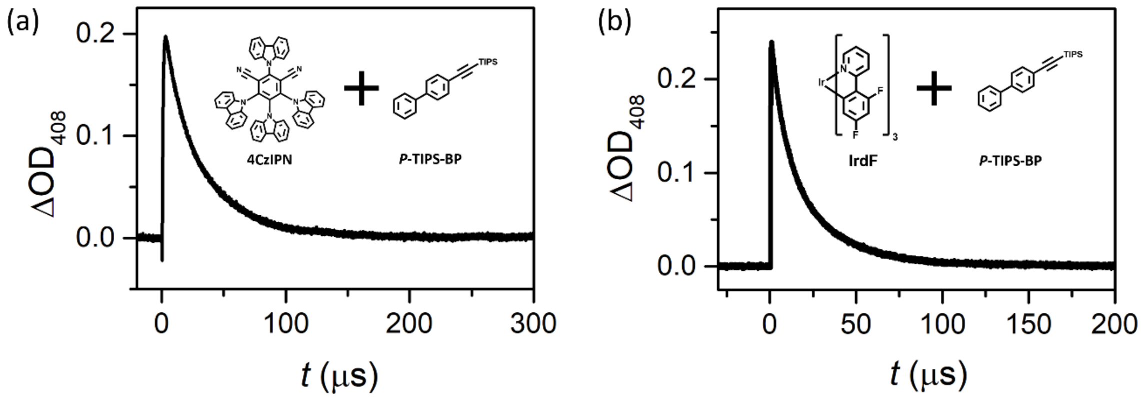

Figure S11: Time-resolved transient absorption measurements of the triplet state formation and decay of ***p*-TIPS-BP** at 408 nm after excitation with 355 nm laser pulses. (a) 20 µM **4CzIPN** with 10 mM ***p*-TIPS-BP** in Ar-saturated cyclohexane:toluene 9:1. (b) 38 µM **IrdF** with 10 mM ***p*-TIPS-BP** in Ar-saturated MeCN.

Comparative LFP experiments on ~20 µM **4CzIPN** solutions (neat cyclohexane or cyclohexane:toluene 9:1) under the conditions as in Figs. 2, 3, 4 and S11 gave practically identical results, regardless of the medium.

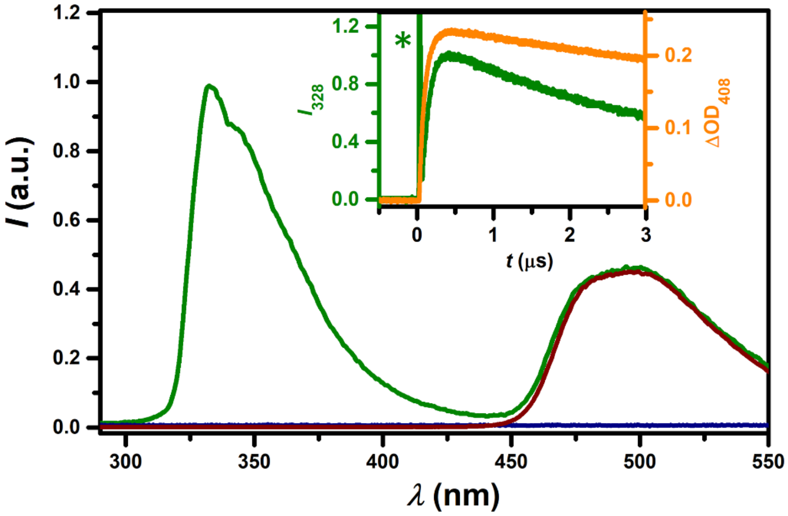

Figure S12: LFP experiments on Ar-saturated MeCN solutions containing 38 µM **IrdF** and/or 10 mM ***p*-TIPS-BP** after excitation with 355 nm laser pulses. Main plot: Normalized time-gated (delay, 1 µs; integration over 200 µs) emission spectra of the complete upconversion system (green), only **IrdF** (brown), and only ***p*-TIPS-BP** (dark blue). Inset: Time-resolved emission (328 nm) and transient absorption (408 nm) traces upon excitation of the UC system. The green asterisk marks laser stray light.

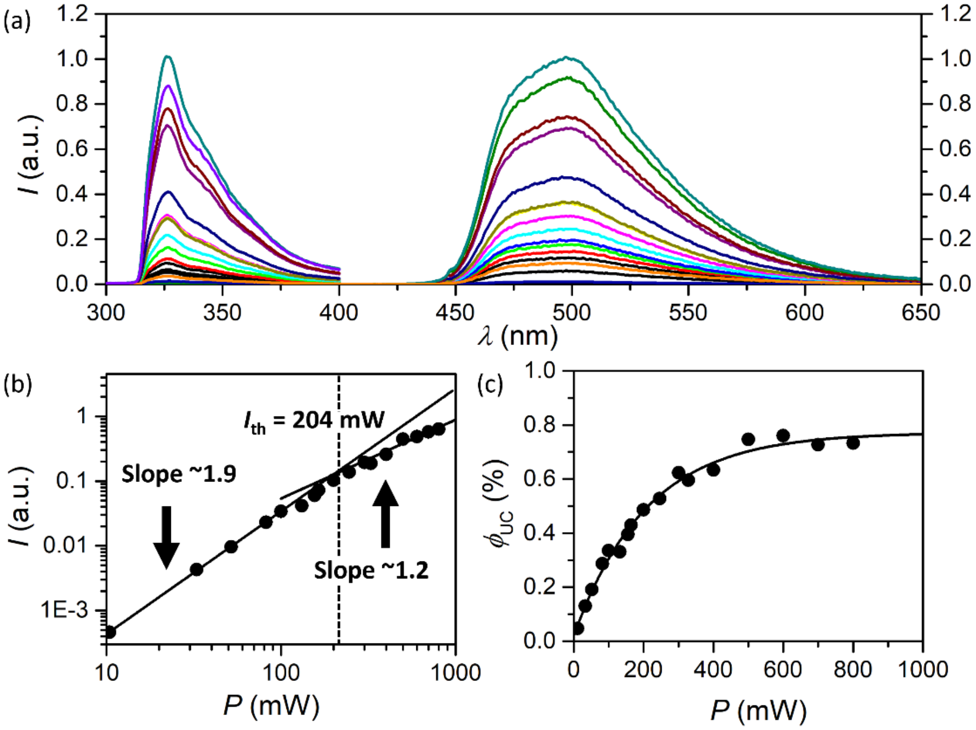

Figure S13: Photon upconversion studies with deoxygenated solutions containing 133 µM **IrdF** and 10 mM ***p*-TIPS-BP** in MeCN using a cw laser for excitation at 447 nm (OD_{447} = 0.1). (a) Main plot: Power-dependent spectra of the normalized upconverted emission and phosphorescence of **IrdF** (reference signal). (b) Normalized UC emission plotted against the laser power on a double-logarithmic scale. The threshold intensity I_{th} was determined by the point of intersection. (c) External quantum yield Φ_{UC} plotted against the laser power.

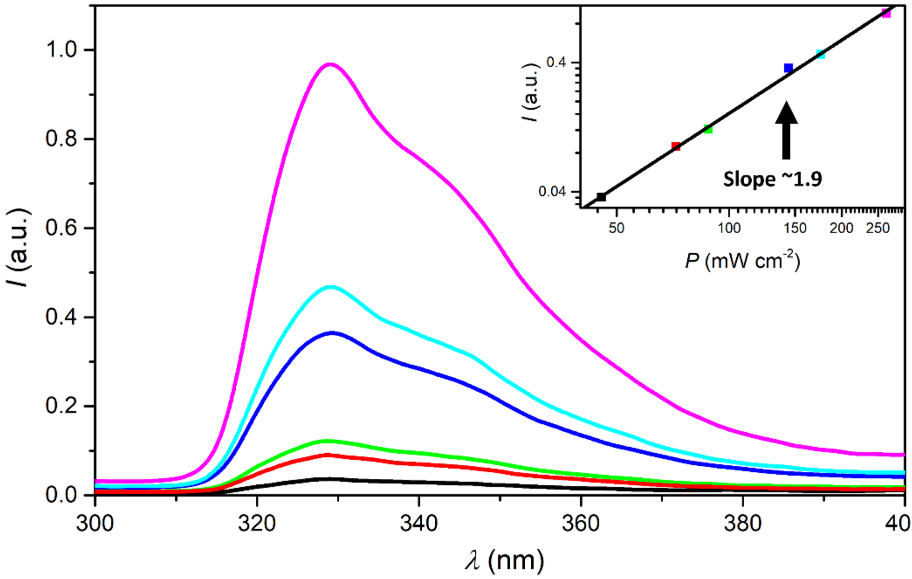

Figure S14: Photon upconversion studies with a deoxygenated solution containing 44 µM **4CzIPN** and 10 mM ***p*-TIPS-BP** in cyclohexane:toluene (9:1) using a blue LED (see Chapter 1 *"general experimental details and methods"* for further information). Inset: Normalized UC emission plotted against the laser power on a double-logarithmic scale.

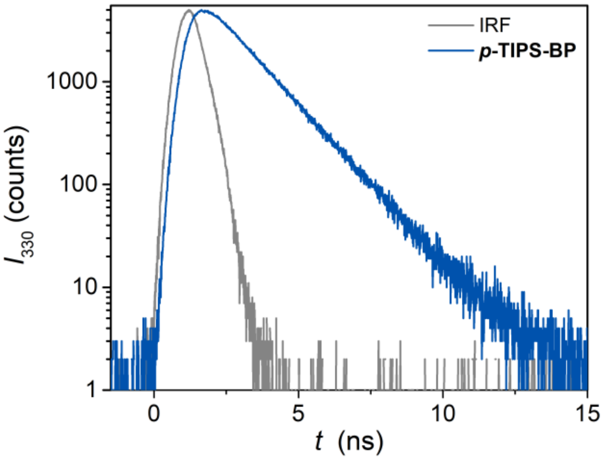

Figure S15: Emission decay of singlet excited ***p*-TIPS-BP** in deoxygenated MeCN upon 313 nm excitation, together with the response function of the TCSPC instrument (IRF, recorded via a stray light measurement with the 313 nm pulsed LED as light source).

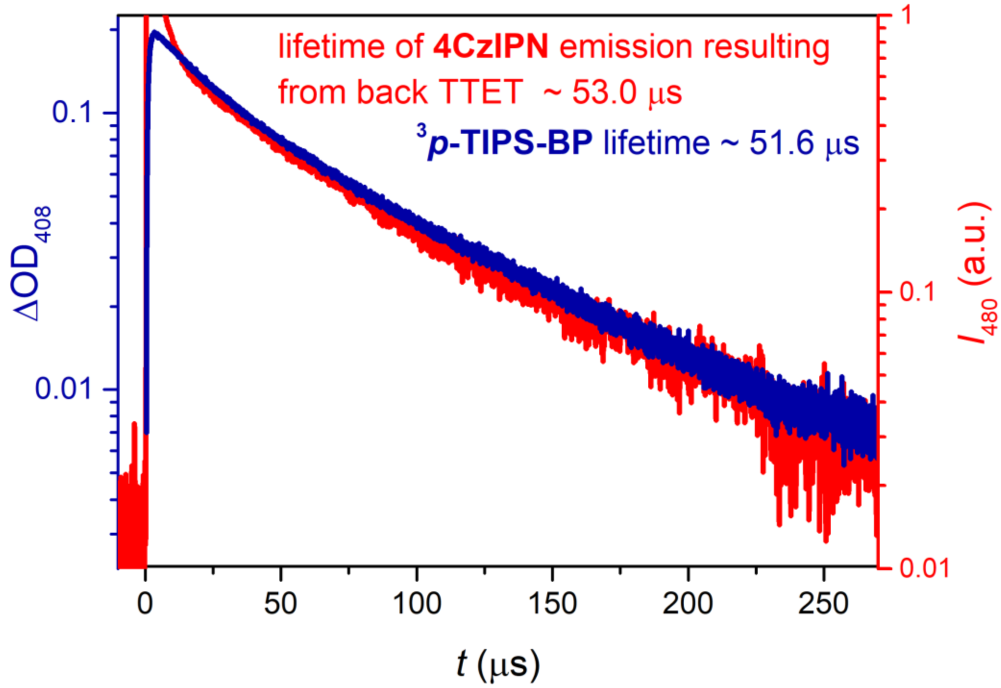

Figure S16: Time-resolved transient absorption and emission measurements (on a logarithmic scale) of a solution containing 10 μM **4CzIPN** with 10 mM ***p*-TIPS-BP** in Ar-saturated cyclohexane:toluene 9:1 after excitation with 355 nm laser pulses. Blue curve: Triplet state decay of ***p*-TIPS-BP** at 408 nm; red curve: Delayed emission of **4CzIPN** as a result of back triplet-triplet energy transfer monitored at 480 nm. A longer ***p*-TIPS-BP** triplet lifetime than in Figure S11 has been observed, which is most likely due to the lower sensitizer concentration slowing down back TTET.

10 NMR spectra

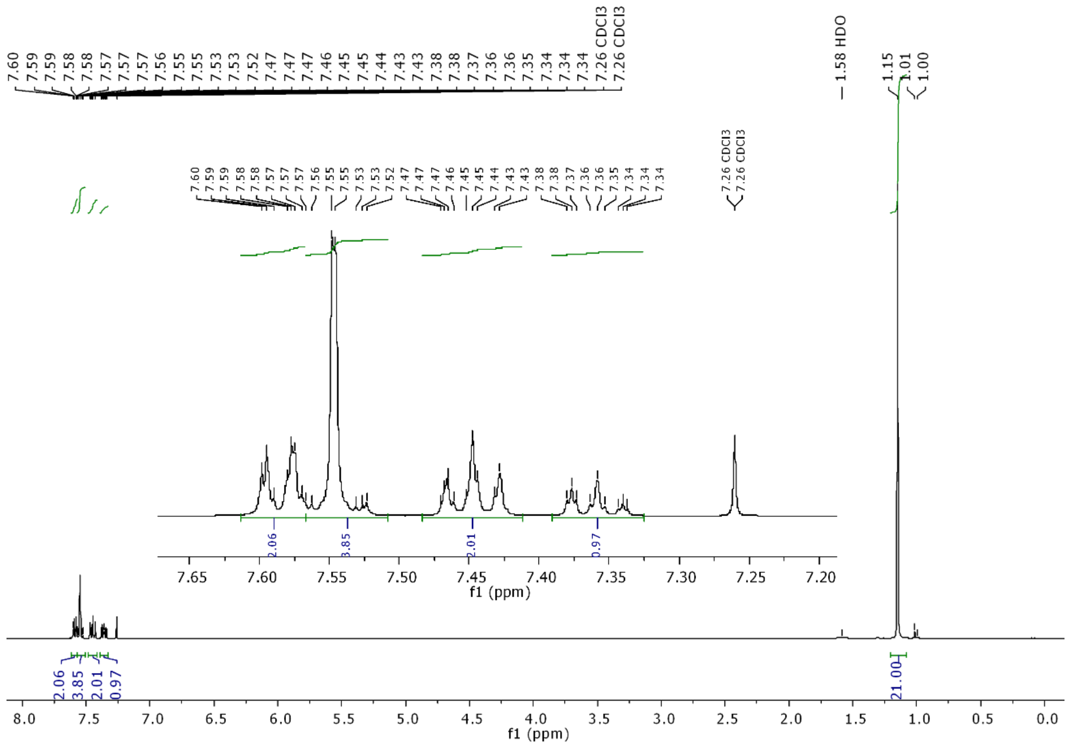

Figure S17: ^{1}H NMR spectrum and zoom into aromatic region (inset) of ***p*-TIPS-BP** in CDCl$_3$.

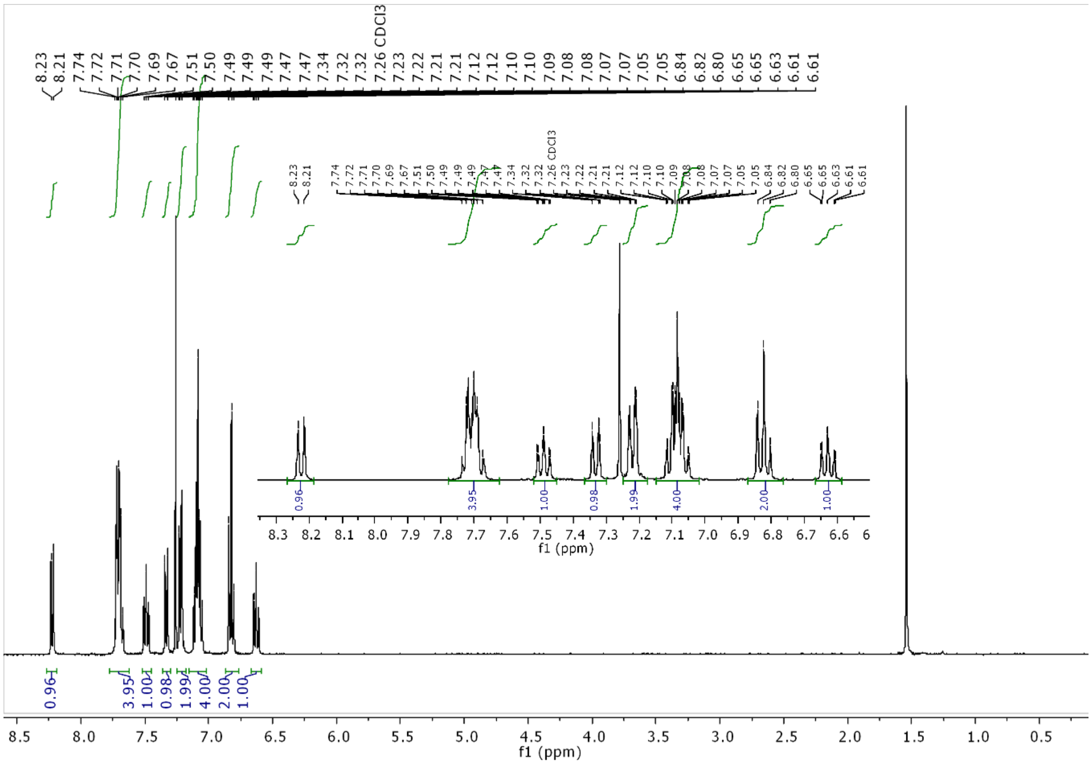

Figure S18: ^{1}H NMR spectrum and zoom into aromatic region (inset) of **4CzIPN** in CDCl$_3$.

11 References

1 M. Montalti, A. Credi, L. Prodi and M. T. Gandolfi, *Handbook of Photochemistry*, CRC Press, 2006.

2 H. Noda, X.-K. Chen, H. Nakanotani, T. Hosokai, M. Miyajima, N. Notsuka, Y. Kashima, J.-L. Brédas and C. Adachi, *Nat. Mater.*, 2019, **18**, 1084–1090.

3 H. Uoyama, K. Goushi, K. Shizu, H. Nomura and C. Adachi, *Nature*, 2012, **492**, 234–238.

4 Kessil PR160L 440 nm, https://www.kessil.com/science/PR160L.php, (accessed 30 September 2021).

5 H. E. Gottlieb, V. Kotlyar and A. Nudelman, *J. Org. Chem.*, 1997, **62**, 7512–7515.

6 N. Harada, Y. Sasaki, M. Hosoyamada, N. Kimizuka and N. Yanai, *Angew. Chem. Int. Ed.*, 2021, **133**, 144–149.

7 B. Feng, Y. Yang and J. You, *Chem. Comm.*, 2020, **56**, 790–793.

8 S. Engle, T. R. Kirkner and C. B. Kelly, *Org. Synth.*, 2019, **96**, 455–473.

9 M. J. Frisch, G. W. Trucks, H. B. Schlegel, G. E. Scuseria, M. A. Robb, J. R. Cheeseman, G. Scalmani, V. Barone, B. Mennucci, G. A. Petersson, H. Nakatsuji, M. Caricato, X. Li, H. P. Hratchian, A. F. Izmaylov, J. Bloino, G. Zheng, J. L. Sonnenberg, M. Hada, M. Ehara, K. Toyota, R. Fukuda, J. Hasegawa, M. Ishida, T. Nakajima, Y. Honda, O. Kitao, H. Nakai, T. Vreven, J. Montgomery, J. A., J. E. Peralta, F. Ogliaro, M. Bearpark, J. J. Heyd, E. Brothers, K. N. Kudin, V. N. Staroverov, R. Kobayashi, J. Normand, K. Raghavachari, A. Rendell, J. C. Burant, S. S. Iyengar, J. Tomasi, M., *Gaussian Inc. Wallingford CT*, 2009.

10 F. M. Hörmann, C. Kerzig, T. S. Chung, A. Bauer, O. S. Wenger and T. Bach, *Angew. Chem. Int. Ed.*, 2020, **59**, 9659–9668.

11 V. Gray, A. Dreos, P. Erhart, B. Albinsson, K. Moth-Poulsen and M. Abrahamsson, *Phys. Chem. Chem. Phys.*, 2017, **19**, 10931–10939.

12 R. Ishimatsu, S. Matsunami, K. Shizu, C. Adachi, K. Nakano and T. Imato, *J. Phys. Chem. A*, 2013, **117**, 5607–5612.

13 Y. Wei, K. Pan, Y. Li, X. Cao, X. Zhou and C. Yang, *Multiple Resonance TADF Sensitizers Enable Green-to-Ultraviolet Photon Upconversion: Application in Photochemical Transformations*, 2021, DOI: 10.33774/chemrxiv-2021-mq00r-v2.

14 Y. Murakami, A. Motooka, R. Enomoto, K. Niimi, A. Kaiho and N. Kiyoyanagi, *Phys. Chem. Chem. Phys.*, 2020, **22**, 27134–27143.

15 P. Duan, N. Yanai and N. Kimizuka, *Chem. Comm.*, 2014, **50**, 13111–13113.

16 I. B. Berlman, *Handbook of fluorescence spectra of aromatic molecules*, Acad. Press, New York, 1971.

17 D. Dzebo, K. Moth-Poulsen and B. Albinsson, *Photochem. Photobiol. Sci.*, 2017, **16**, 1327–1334.

18 J. Ma, S. Chen, C. Ye, M. Li, T. Liu, X. Wang and Y. Song, *Phys. Chem. Chem. Phys.*, 2019, **21**, 14516–14520.

19 C. Kerzig and O. S. Wenger, *Chem. Sci.*, 2018, **9**, 6670–6678.